COMPACT LOWPASS FILTER WITH WIDE STOPBAND BANDWIDTH

Xianhong Chen, Lijun Zhang, Yatao Peng, Yongqing Leng, Hui Lu, and Zhanqi Zheng
Institute of Microelectronics, Chinese Academy of Sciences, Beitucheng West Road, Beijing 100029, China; Corresponding author: chenxianhong@ime.ac.cn

Received 19 June 2014

ABSTRACT: *A compact microstrip lowpass filter (LPF) which consists of a meander line, a coupled line and two open stubs is proposed. The mechanism for reallocating filter transmission zeros and the design procedure are explained. The simulated and measured results demon-strate that this LPF provides compact size, low insertion loss, and wide stopband.* Microwave Opt Technol Lett 57:367–371, 2015; View this article online at wileyonlinelibrary.com. DOI 10.1002/mop.28853

Key words: *lowpass filter; transmission zero; meander line; open stubs*

1. INTRODUCTION

Compact lowpass filters (LPF) with high performance are in great demand for communication systems to suppress harmonics and spurious signals. The conventional stepped impedance and open-stub LPFs suffer from gradual cutoff and narrow stopband bandwidth [1]. To address these problems, conventional filters require more sections, which unfortunately increases the filter size and insertion loss [2]. Defected ground structures (DGS) have been used in [3] to obtain wide stopband. However, DGS

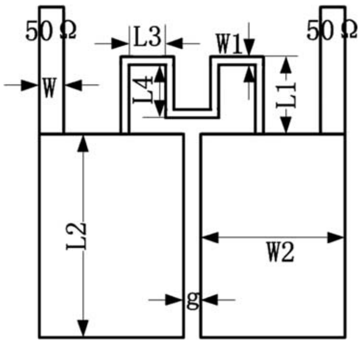

Figure 1 The schematic of the proposed LPF without open stubs, denoted as LPF1

requires a special package which increases the fabrication difficulties. A compact semilumped LPF was also proposed in [4]. However, the use of lumped elements is restricted by the frequency because of the parasitic effect. LPFs constructed by a hairpin-shaped unit [2,5] and [6] have small size, but their stopband bandwidth is narrow. By adding open stubs, wide stopband bandwidth is obtained in [7–9], but the stubs enlarge the filter area.

In this letter, a very compact LPF is achieved by combining a meander line and a coupled line. Upper stopband is expanded by adding two shunt open stubs with the filter area almost unchanged. Closed-form design formulations are first established to reallocate the transmission zeros of the proposed filter with open stubs. These equations show that five transmission zeros can be produced when the admittance ratio is >1.The design procedure is then given. At last, LPFs with/without open stubs are designed with 1.2 GHz cutoff frequency. Measured results validate the theory of the LPF.

2. FILTER TRANSMISSION ZEROS

Figure 1 shows the schematic of the proposed LPF without open stubs, hereafter denoted as LPF1. LPF1 can create three transmission zeros f_{z1}, f_{z2}, and f_{z3} at most.

Figure 2 shows LPF1's transmission-line model and π -type equivalent circuit with lumped elements. Y_{0e} and Y_{0o} are the even- and odd-mode characteristic admittances of the coupled lines whose electrical lengths are θ. The total electrical lengths of the meander lines are 2θ and the characteristic admittance is Y_t.

Using the lossless transmission-line model, the lumped elements in Figure 2 are obtained in [6] as

$$j\omega L_t = j\sin(2\theta)/Y_t, \tag{1a}$$

$$j\omega C_t = jY_t \tan\theta, \tag{1b}$$

$$j\omega C_g = j\tan\theta (Y_{0o} - Y_{0e})/2, \tag{1c}$$

$$j\omega C_c = jY_{0e}\tan\theta. \tag{1d}$$

The equivalent circuit of the proposed LPF can be expressed in Figure 3(a). To have low-pass characteristic, Figure 3(a) should be equal to the prototype LPF as shown in Figure 3(b). The condition of the equivalence between Figures 3(a) and 3(b) can be easily derived as follow

$$j\omega C_1 = j(Y_{0e} + Y_t)\tan\theta, \tag{2a}$$

$$1/(j\omega L_2) = j0.5(Y_{0o} - Y_{0e} - Y_t)\tan\theta - j0.5 Y_t \cot\theta. \tag{2b}$$

The ABCD-matrix of the LPF prototype is

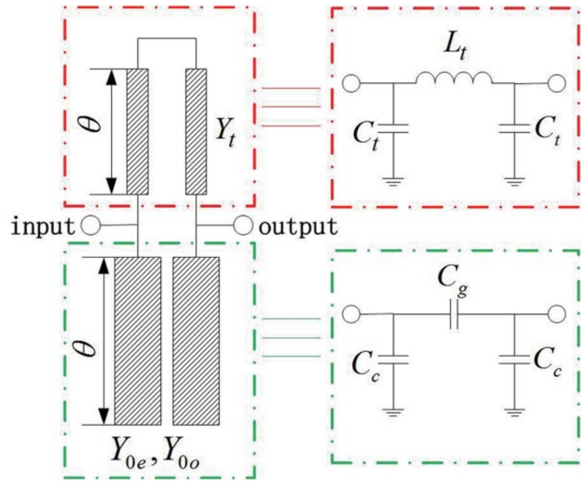

Figure 2 Equivalent transmission-line model of LPF1 and its equivalent circuit with lumped elements. [Color figure can be viewed in the online issue, which is available at wileyonlinelibrary.com]

$$\begin{bmatrix} A & B \\ C & D \end{bmatrix} = \begin{bmatrix} 1 + Y_1/Y_2 & 1/Y_2 \\ 2Y_1 + Y_1^2/Y_2 & 1 + Y_1/Y_2 \end{bmatrix} \tag{3}$$

With $Y_1 = j\omega C_1$ and $Y_2 = 1/(j\omega L_2)$.

To improve the stopband rejection, two open stubs $(Z_s, \theta_{s1}; Z_s, \theta_{s2})$ are added like [7,8] as shown in Figure 4, hereafter denoted as LPF2. The open stubs introduce two additional transmission zeros f_{z4} and f_{z5}. LPF2 can be seen as three networks connected in cascade, thus, the overall ABCD-matrix is calculated by simple matrix multiplication of the three ABCD-matrices

$$\begin{bmatrix} A' & B' \\ C' & D' \end{bmatrix} = \begin{bmatrix} 1 & 0 \\ j0.5\tan\theta_{s1} & 1 \end{bmatrix} \begin{bmatrix} A & B \\ C & D \end{bmatrix} \begin{bmatrix} 1 & 0 \\ j0.5\tan\theta_{s2} & 1 \end{bmatrix}. \tag{4}$$

Then, the transmission coefficient (S_{21}) of LPF2 can be derived as

$$\begin{aligned} S_{21} = 4Y_0Y_2/(&4(Y_0Y_1 + Y_0Y_2 + Y_1Y_2) + 2(Y_0^2 + Y_1^2) \\ &+ j(\tan\theta_{s1} + \tan\theta_{s2})(Y_0 + Y_1 + Y_2) - 0.5\tan\theta_{s1}\tan\theta_{s2}) \end{aligned} \tag{5}$$

where Y_0 is the characteristic admittance of the feed lines.

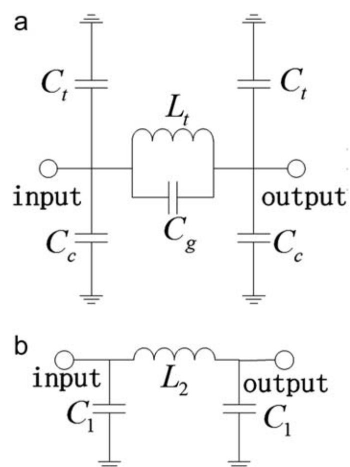

Figure 3 (a) The equivalent circuit of the proposed LPF. (b) The LPF prototype

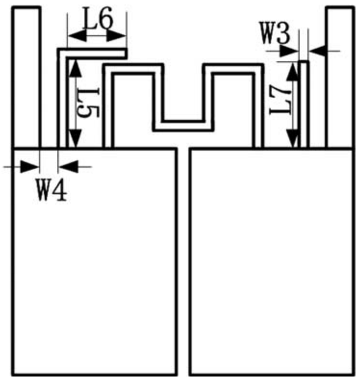

Figure 4 The schematic of the proposed LPF with open stubs, denoted as LPF2

Under the condition of $S_{21}=0$, all the transmission zeros can be determined from (4) as

$$\theta=(\pi/2)(2n+1), \tag{6a}$$

$$\theta=\cot^{-1}(\pm\sqrt{R-1}), \tag{6b}$$

$$\theta_{s1}=(\pi/2)(2n+1), \tag{6c}$$

$$\theta_{s2}=(\pi/2)(2n+1), \tag{6d}$$

where $R=(Y_{0o}-Y_{0e})/Y_t$ is the admittance ratio and n is the integer number.

Transmission zeros f_{z1} and f_{z3} are given in (6b) when the admittance ratio $R>1$. f_{z2} is determined by (6a). The variation of transmission zero positions with the admittance ratio R is plotted in Figure 5(a). As R increases, the space between f_{z1} and f_{z3} is expanded. Figure 5(b) shows S_{21} with respect to the frequency under varied admittance ratio R. It reveals that, as R increases, the stopband between f_{z1} and f_{z3} is expanded at the cost of increasing the ripple between f_{z2} and f_{z3}.

The transmission zeros (f_{z4},f_{z5}) due to the two open stubs are given by (6c) and (6d). The positions of f_{z4} and f_{z5} can be tuned by choosing different electrical lengths θ_{s1} and θ_{s2}, respectively. If one of the stubs produces transmission zero near $2f_{z2}$, it can suppress the second harmonic passband of LPF1 [10], thus, the overall stopband is expanded.

Equation (6) also shows that, the positions of f_{z1}, f_{z2}, and f_{z3} have no relation with the positions of f_{z4} and f_{z5}.

3. FILTER PROTOTYPE AND DESIGN PROCEDURE

To illustrate the design procedure for the proposed filter, a three-pole lowpass prototype is chosen, whose element values are g_0, g_1, g_2, g_3, g_4 when the cutoff frequency is 1 rad. Based on the element transformations [1], the lumped elements in Figure 3 are

$$C_1=g_0g_1Y_0/\omega_c, \tag{7a}$$

$$L_2=g_2/(g_0Y_0\omega_c) \tag{7b}$$

Based on the derived results in Figrue 5, choose transmission zeros f_{z1}, f_{z2}, and f_{z3} as (8) so as to get wider stopband and keep the insertion loss in the whole stopband higher.

$$f_{z2}=4.5f_c \text{ such that } \theta=\pi/9@f_c, \tag{8a}$$

$$(Y_{0o}-Y_{0e})/Y_t=R=2 \text{ such that } f_{z1}=2.25f_c, f_{z3}=6.75f_c, \tag{8b}$$

where f_c is the 3 dB cutoff frequency.

f_{z4} is set between f_{z2} and f_{z3} to reduce the ripple. f_{z5} is set near $2f_{z2}$ to suppress the second harmonic passband of LPF1.

$$f_{z4}=6f_c \text{ such that } \theta_{s1}=\pi/12\,@f_c, \tag{9a}$$

$$f_{z5}=8f_c \text{ such that } \theta_{s2}=\pi/16\,@f_c. \tag{9b}$$

With (7), (8), (9), and (2), Y_{0o}, Y_{0e}, Y_t and $\theta, \theta_{s1}, \theta_{s2}$ can be derived to settle most of the filter dimensions. Then, the dimensions can be tuned to achieve good performance.

4. FABRICATION AND RESULT DISCUSSION

Based on the design procedure, LPF1 and LPF2 are designed and fabricated on Rogers RO4350 with relative permittivity is 3.5 and thickness is 0.762 mm. Choose the lowpass prototype as $g_0=g_1=g_3=g_4=1$, $g_2=2$, and the 3 dB cutoff frequency at 1.2 GHz. $Y_t=0.0084$, $Y_{0e}=0.0465$, $Y_{0o}=0.0633$, $\theta=\pi/9$, $\theta_{s1}=\pi/12$, $\theta_{s2}=\pi/16$ can be obtained to determine some of the theoretical filter dimensions. The theoretical and optimized dimensions of the LPFS are list in Table 1 (unit: mm), where L is the total length of meander line as $L=2L1+3L3+2L4$.

Figure 6(a) is the photograph of the fabricated LPF1. Figure 7(a) is the measured S-parameters and simulated S-parameters based on the ADS momentum model. The measured 3 dB cutoff frequency of LPF1 is 1.2 GHz. Its stopband extends from 1.80

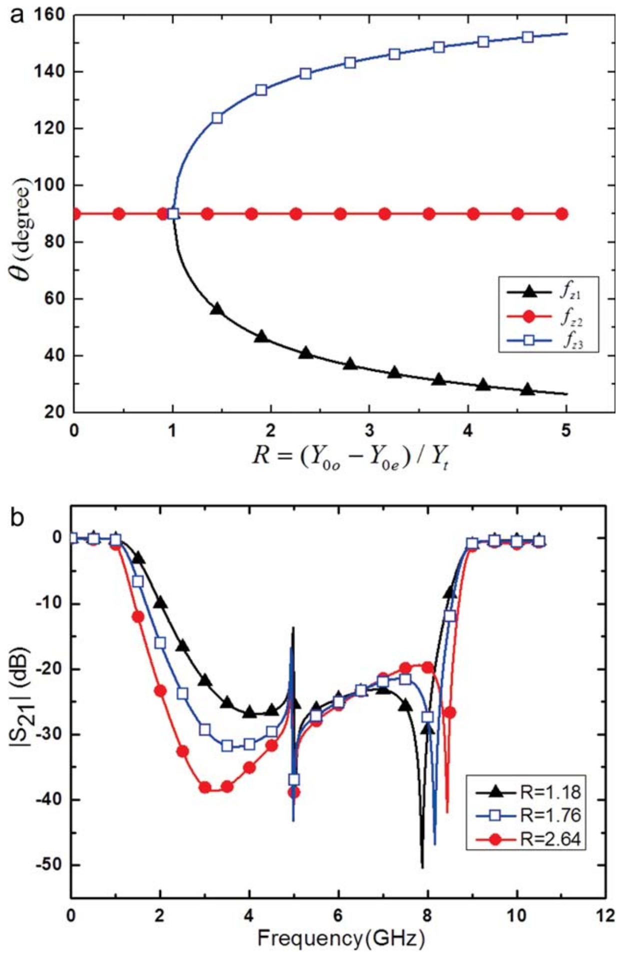

Figure 5 Transmission zeros characteristics of LPF1. (a) Transmission zero positions with different R. (b) S_{21} with respect to the frequency under varied admittance ratio ($L1=4.13$, $L2=8.64$, $L3=1.68$, $L4=2.82$, unit: mm). [Color figure can be viewed in the online issue, which is available at wileyonlinelibrary.com]

TABLE 1 Theoretical and Optimized Dimensions of the LPFS

	$W1$	$W2$	$L2$	L	g	$L7$	$L5+L6$
Theory	0.21	6.03	7.84	17.70	0.14	4.98	6.63
LPF1	0.30	6.50	8.64	18.94	0.15	–	–
LPF2	0.21	7.01	7.41	16.60	0.15	4.46	6.60

to 8.42 GHz under the insertion loss >15 dB. The return loss in passband is >16 dB. The physical size of LPF2 is about 13.15 mm × 12.77 mm ($0.098\lambda_c \times 0.096\lambda_c$, the guided wavelength λ_c corresponds to that of a 50 Ω line at 1.2 GHz). LPF1 has three transmission zeros at 2.8, 4.8, and 7 GHz. The zero at 4.8 GHz is not so distinct, because there is a transmission pole nearby.

Figures 6(b) and 7(b) show the photograph and S-parameters of the fabricated LPF2, respectively. Its 3 dB cutoff frequency is also 1.2 GHz. The stopband has been expanded from 1.91 to 10.35 GHz with insertion loss >15 dB. The return loss in passband is >17 dB. The physical size is about 14.17 mm × 12 mm ($0.106\lambda_c \times 0.090\lambda_c$) which is almost the same with the size of LPF1. The two open stubs introduce transmission zeros at 6.5 and 9.2 GHz, respectively. The zero at 6.5 GHz reduces the ripple and the one at 9.2 GHz expands the stopband.

Table 2 shows the comparison results between the proposed LPFs and other LPFs. The data of other LPFs is sorted out by [8]. The sizes of our LPFs are most compact. The stopbands are wider than others except [8]. Return loss in passband of LPF2 is better than others except [11].

5. CONCLUSION

This article introduces a compact and wide rejection bandwidth LPF composed of a pair of coupled lines, a meander line, and two shunt open stubs. The two stubs are added with the filter area almost unchanged. The mechanism for reallocating transmission zeros of the proposed filter is explained and show that five transmission zeros can produced when the admittance ratio is >1. At last, LPFs with/without open stubs has been fabricated with good lowpass performance. The LPF with open stubs has achieved up to 8.6th harmonic rejection better than 15.0 dB. The return loss in the passband is more than 17 dB. The circuit size is $0.106\lambda_c \times 0.090\lambda_c$.

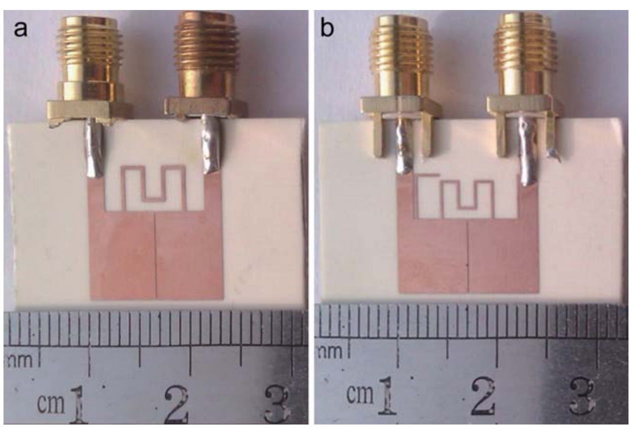

Figure 6 (a) Photograph of the designed LPF1 ($W = 1.62$, $W1 = 0.30$, $W2 = 6.50$, $L1 = 4.13$, $L2 = 8.64$, $L3 = 1.5$, $L4 = 2.82$, $g = 0.15$, unit: mm). (b) Photograph of the designed LPF2 ($W = 1.62$, $W1 = 0.21$, $W2 = 7.01$, $L1 = 3.63$, $L2 = 7.41$, $L3 = 1.68$, $L4 = 2.42$, $g = 0.15$, $W3 = 0.21$, $W4 = 0.2$, $L5 = 4.30$, $L6 = 2.30$, $L7 = 4.49$, unit: mm). [Color figure can be viewed in the online issue, which is available at wileyonlinelibrary.com]

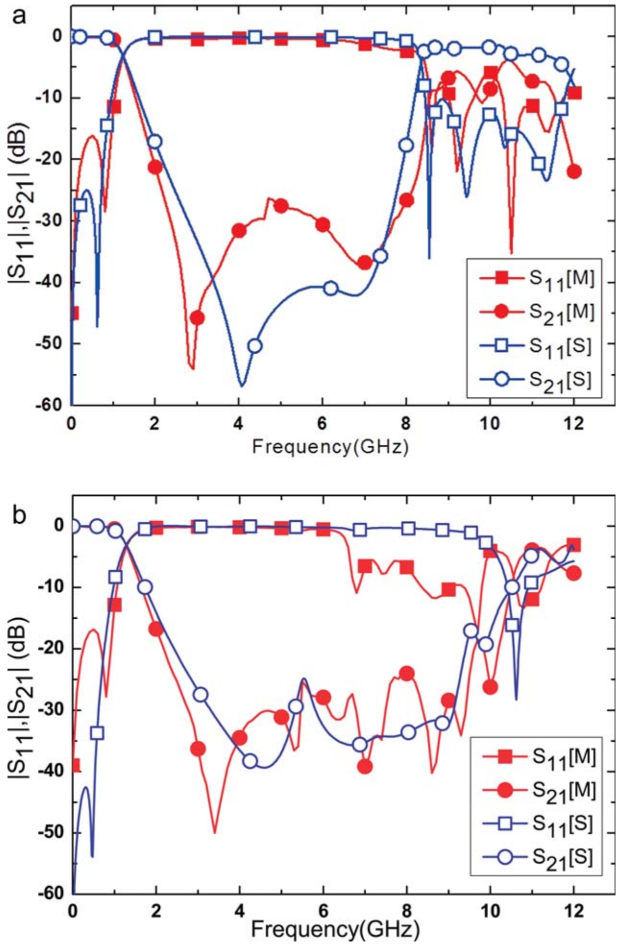

Figure 7 (a) Measured and simulated S-parameters of LPF1. (b) Measured and simulated S-parameters of LPF2. [Color figure can be viewed in the online issue, which is available at wileyonlinelibrary.com]

TABLE 2 Compared with Other LPFS

Ref.	f_c (GHz)	Min. RL (dB)	Stopband Up to (f_c)	Stopband 15dB FBW	Circuit Size (λ_g^2)
[2]	2	13.6	5	1.16	Large
[9]	2.4	15	3.4	1.13	0.049
[10]	2.5	14	4.8	1.20	0.022
[11]	1	20	6	1.26	0.012
[8]	0.5	16.3	9	1.44	0.022
LPF1	1.2	16	7	1.30	0.0094
LPF2	1.2	17	8.6	1.38	0.0095

FBW=fractional bandwidth; Min. RL=minimum return loss.

ACKNOWLEDGMENTS

This research is supported by the National Basic Research Program of China under 973 Program 2010CB327506.

REFERENCES

1. J.S. Hong and M.J. Lancaster, Microstrip filters for RF/microwaveapplications, Wiley, New York, 2001.
2. H. Lung-Hwa and C. Kai, Compact elliptic-function low-pass filters using microstrip stepped-impedance hairpin resonators, IEEE Trans Microwave Theory Tech 51 (2003), 193–199.
3. A. Dal, P. Jun-Seok, K. Chul-Soo, K. Juno, Q. Yongxi, and T. Itoh, A design of the low-pass filter using the novel microstrip defected ground structure, IEEE Trans Microwave Theory Tech 49 (2001), 86–93.

4. J.-W. Sheen, A compact semi-lumped low-pass filter for harmonics and spurious suppression, Microwave Guid Wave Lett 10 (2000), 92–93.
5. K. Jen-Tsai and S. Jason, A compact distributed low-pass filter with wide stopband, In: 2001 Asia-Pacific Microwave Conference, Taipei, Taiwan, 2001. APMC 2001, vol. 1, 2001, pp. 330–333.
6. Y.-W. Lee, C. Sung-Min, K. Geun-Young, P. Jun-Seok, A. Dal, and J.-B. Lim, A design of the harmonic rejection coupled line low-pass filter with attenuation poles, In: 1999 Asia Pacific Microwave Conference, vol. 3, 1999, pp. 682–685.
7. W. Feng, C. Lei, and S. Xiao-Wei, Compact lowpass filter based on coupled-line hairpin unit, Electron Lett 48 (2012), 379–381.
8. V.K. Velidi and S. Sanyal, Sharp roll-off lowpass filter with wide stopband using stub-loaded coupled-line hairpin unit, Microwave Wireless Compon Lett 21 (2011), 301–303.
9. Y. Jinping and W. Wen, Compact elliptic-function low-pass filter using defected ground structure, IEEE Microwave Wireless Compon Lett 18 (2008), 578–580.
10. S. Luo, L. Zhu, and S. Sun, Stopband-expanded low-pass filters using microstrip coupled-line hairpin units, IEEE Microwave Wireless Compon Lett 18 (2008), 506–508.
11. L. Lin, L. Zheng-Fan, and M. Jun-Fa, Compact lowpass filters with sharp and expanded stopband using stepped impedance hairpin units, Microwave Wireless Compon Lett 20 (2010), 310–312.